Retinal Binding during Folding and Assembly of the Membrane Protein Bacteriorhodopsin†

Paula J. Booth,*,‡,§ Amjad Farooq,‡,§ and Sabine L. Flitsch‖,⊥

Department of Biochemistry and Dyson Perrins Laboratory, University of Oxford, Oxford OX1, U.K.

Received January 18, 1996; Revised Manuscript Received March 5, 1996⊗

ABSTRACT: The factors driving folding and assembly of integral membrane proteins are largely unknown. In order to determine the role that the retinal chromophore plays in assembly of bacteriorhodopsin, we have determined the kinetics and thermodynamics of retinal binding during regeneration of bacteriorhodopsin, from denatured apoprotein, *in vitro*. Regeneration is initiated by rapid, stopped-flow, mixing of the denatured apoprotein bacterioopsin in sodium dodecyl sulfate micelles with mixed detergent/lipid micelles containing retinal. Regeneration kinetics are measured by time-resolving changes in protein fluorescence. The dependence of each kinetic component on retinal concentration is determined. Only one experimentally observed rate constant is dependent on retinal concentration, leading to identification of only one second-order reaction involving retinal and bacterioopsin. This reaction occurs after a rate-limiting step in bacterioopsin folding, and results in formation of a noncovalent retinal/protein complex. The free energy change of this retinal binding step is determined, showing that thermodynamic information can be obtained on transient intermediates involved in membrane protein regeneration.

The correct assembly of proteins which are integral to biological membranes is vital for membrane function. Like most proteins, membrane proteins are unable to function unless folded into a specific, three-dimensional shape. Although there has been progress toward understanding this precise folding for water-soluble proteins (Matthews, 1993), there is little information for integral membrane proteins. Bacteriorhodopsin provides an ideal model system for a study of membrane protein folding kinetics (Huang et al., 1981; London & Khorana, 1982; Booth et al., 1995). This integral membrane protein is the only protein present in the purple membrane of *Halobacteria salinaria*, where it functions as a light-driven proton pump (Stoeckenius & Bogomolni, 1982).

Bacteriorhodopsin is one of the few membrane proteins for which a high-resolution structure is known (Henderson et al., 1990). The protein is 248 amino acids long and consists of 7 transmembrane helices connected by short extramembranous loops. A retinal chromophore is covalently bound within the seven helix bundle via a protonated Schiff-base linkage to Lys-216. Bacteriorhodopsin is part of a family of retinal binding proteins which includes the mammalian vision receptor rhodopsin, and for which it is often used as a model system (Oesterhelt & Tittor, 1989; Khorana, 1993). The function of both bacteriorhodopsin and rhodopsin is reliant on photoisomerization of retinal. Retinal undergoes thermal reisomerization while remaining bound to bacteriorhodopsin; however, in the case of rhodopsin, retinal has to be expelled from its binding site for reisomerization (Birge, 1990). Thus, incorporation of retinal and regeneration of rhodopsin are key to the action of the vision receptor. Indeed, the action of many membrane-bound receptors is dependent on the binding of a small molecular cofactor which in the case of G-protein receptors is an agonist or antagonist. Rhodopsin itself is a member of the large family of G-protein receptors (Hargrave, 1991). These receptors seem to possess structures which, although not identical to that of bacteriorhodopsin, are based on seven transmembrane helices (Hargrave, 1991; Schertler et al., 1993; Donnelly & Findlay, 1994). It has been speculated by analogy with the retinal binding proteins that the seven helices of the G-protein receptors also form their cofactor binding pockets, giving binding pockets that are surprisingly similar, in view of the variety of cofactor structure and the fact that rhodopsin is the only G-protein receptor to bind its cofactor covalently (Oprian, 1992; Savarese & Fraser, 1992).

Bacteriorhodopsin can be spontaneously refolded to a native state from a denatured state *in vitro* (Huang et al., 1981; London & Khorana, 1982), allowing its assembly kinetics to be studied (London & Khorana, 1982; Booth et al., 1995). Indeed, it is one of the few membrane proteins for which this is possible; to date, spontaneous refolding has only been shown for two other membrane proteins: porins (Eisele & Rosenbuch, 1990) and the major light-harvesting complex of green plants (Plumley & Schmidt, 1987; Paulsen et al., 1990). Bacteriorhodopsin can be refolded from a denatured state to a state with native secondary structure in the absence of retinal (London & Khorana, 1982; Popot et al., 1987), implying that retinal does not initiate protein folding. Addition of retinal to this partially folded state regenerates bacteriorhodopsin, in a reaction that consists of at least two stages: first, noncovalent binding of retinal in its binding site; and second, formation of the Schiff base (London & Khorana, 1982; Popot et al., 1987; Booth et al.,

† This work was supported by the BBSRC (studentship to A.F. and Grant GR/J67857) and the Royal Society. P.J.B. is Rosenheim Research Fellow of the Royal Society.

* To whom correspondence should be addressed.

‡ Department of Biochemistry.

§ Present address: Department of Biochemistry, Imperial College of Science, Technology & Medicine, London, SW7 2AY, U.K.

‖ Dyson Perrins Laboratory.

⊥ Present address: Chemistry Department, University of Edinburgh, Edinburgh EH9 3JJ, U.K.

⊗ Abstract published in *Advance ACS Abstracts,* April 15, 1996.

S0006-2960(96)00129-8 CCC: $12.00

1995). Retinal binding to bleached purple membrane, or bleached, monomeric, bacteriorhodopsin, also seems to occur in two similar stages (Oesterhelt et al., 1973; Oesterhelt & Schuhmann, 1974; Schreckenbach et al., 1977).

We have recently reported a kinetic study of bacteriorhodopsin assembly with millisecond time resolution (Booth et al., 1995). Folding was initiated by a stopped-flow method, whereby a denatured state of bacteriorhodopsin, in sodium dodecyl sulfate (SDS)[1] detergent micelles, was rapidly mixed with renaturing, mixed dimyristoylphosphatidylcholine (DMPC)/CHAPS micelles containing retinal (Booth et al., 1995). Changes in protein fluorescence were used to follow protein folding and assembly. These experiments indicated several kinetic phases to the regeneration. A very fast, 250 s^{-1}, phase accompanied mixing of the SDS and DMPC/CHAPS micelles, while phases of the order of 1.2−2.0 and 0.067 s^{-1} were assigned to formation of partially folded apoprotein intermediates (I_1 and I_2). Other phases were resolved for retinal binding, about 2.0 s^{-1} for noncovalent binding, and 0.02 and 0.0014 s^{-1} for subsequent Schiff-base formation. The following, tentative, reaction scheme for bacteriorhodopsin regeneration was suggested: bO → I_1 → I_2 → I_R → bR. I_2 was presumed to correspond to the state with native secondary structure which accumulates in the absence of retinal (London & Khorana, 1982), and retinal was proposed to bind only to I_2, resulting in formation of a noncovalent, retinal/protein intermediate, I_R. However, it was not possible to rule out that retinal bound earlier during assembly (for example to I_1, or before all secondary structure has formed), nor to confirm that I_1 and I_2 were formed sequentially. In addition, the use of fluorescence spectroscopy to monitor changes in protein fluorescence during folding and regeneration gives little information on associated protein structural changes. However, if thermodynamic information on transient regeneration intermediates can be obtained, this can be combined with site-directed mutagenesis methods to give information on the structures of intermediates (Bycroft et al., 1990; Matouschek et al., 1990).

Here, we show how thermodynamic information can be obtained on intermediates involved in bacteriorhodopsin regeneration by investigating the role that retinal plays in the regeneration process. In order to identify retinal binding step(s), we have investigated the dependence of each regeneration kinetic on retinal concentration. Addition of retinal at different times during protein folding and assembly confirms that retinal binding is preceded by a slower, protein folding event. These studies identify only one second-order retinal, protein reaction, confirming that retinal only binds to the intermediate I_2. The free energy of this retinal binding reaction can be estimated, giving information on the role that retinal plays in driving regeneration of bacteriorhodopsin.

MATERIALS AND METHODS

Materials. L-α-1,2-Dimyristoylphosphatidylcholine (DMPC) was obtained from Avanti Phospholipids, 3-[(3-cholamidopropyl)dimethylammonio]-1-propanesulfonate (CHAPS) was from Calbiochem, and SDS (electrophoresis grade) and *all-trans*-retinal were from Sigma. All other reagents and chemicals were of analytical grade.

Mixed DMPC/CHAPS micelles were prepared by stirring 2% (w/v) DMPC in 50 mM sodium phosphate buffer, pH 6, for 2 h at room temperature. CHAPS was then added to 2% (w/v) final concentration and the mixture sonicated in a bath sonicator for 30 min. The resulting clear, micellar solution could be stored at 4 °C for several days.

Retinal was dissolved in ethanol (Analar), and the concentration was determined from the absorbance at 380 nm using an extinction coefficient of 42 800 cm^{-1} M^{-1} (Rehorek & Heyn, 1979). Retinal was stored in ethanol at −70 °C, in the dark under argon, for up to 1 month. Retinal was always handled in dim or red light.

Preparation of Bacterioopsin. Bacteriorhodopsin was isolated as purple membrane from *Halobacterium salinarium* (strain S9) according to the method of Oesterhelt and Stoeckenius (1974). The strain was maintained on plates of the growth medium containing 2% agar, and transferred every 2 or 3 months. Plates were incubated at 37 °C for 2 weeks, and stored at 4 °C. Liquid/shake cultures were grown directly from bright purple colonies, at 37 °C in the dark, in medium containing Oxoid peptone; 700 mL cultures (inoculated with about 50 mL) were shaken in 2 L flasks at 100−120 rpm, and cells were harvested after about 3−4 days when absorbances at 560 and 660 nm were 1.5−2 and 1−1.5, respectively (late log phase). Sucrose density gradients were run on all-purple membrane preparations, which were then stored at 4 °C as an aqueous suspension (20−40 mg·mL^{-1}), containing 0.025% azide. Typical yields of purified purple membrane were 20 mg·L^{-1}.

Delipidated, denatured bacterioopsin (bO) in SDS was prepared from purple membrane by the method of Braiman et al. (1987). Briefly, an aqueous suspension of purple membrane was mixed with an organic solvent containing chloroform/methanol/triethylamine (100:100:1 volume ratio) to achieve a single phase (solvent/aqueous suspension, about 8:1). Hydroxylamine was added to remove retinal, and phase separation was effected by addition of a buffer containing 0.1 M phosphate, pH 6.0 (buffer to solvent volume ratio, about 1:1). Delipidated bO was recovered as described (Braiman et al., 1987). Phase separation and recovery of the protein interphase were repeated twice. The final wet pellet of delipidated bO was taken up directly in an aqueous solution of SDS (5% w/v) to give a final SDS:protein ratio (w/w) of 5:1 (SDS concentration about 1% w/v). This required vigorous stirring to disperse the wet bO pellet, followed by centrifugation to remove any insoluble material. The final SDS-solubilized bO was stored at −20 °C. Alternatively, the wet bO pellet was transferred to SDS by redissolving the pellet in the minimum volume of chloroform/methanol/triethylamine solvent, and then adding aqueous SDS. The solvent was then evaporated in a SAVANT SPEEDVAC and the dry powder stored at −20 °C. Several bO preparations were obtained from one preparation of purple membrane. About 50% of the protein present in the purple membrane was recovered as bO in SDS.

All procedures involving organic solvents were done in clean, dry glassware.

Steady-State Spectroscopy. Absorption measurements were made with a UVIKON 930 or Aminco DW2000 spectrophotometer with a 2 nm bandwidth and 1 cm path length. Fluorescence measurements were made with a Perkin

[1] Abbreviations: bO, bacterioopsin; CHAPS, 3-[(3-cholamidopropyl)dimethylammonio]-1-propanesulfonate; DMPC, L-α-1,2-dimyristoylphosphatidylcholine; FWHM, full width half-maximum; SDS, sodium dodecyl sulfate.

Elmer LS50 spectrometer, with excitation at 290 nm, and excitation and emission bandwidths of 2.5 nm. Fluorescence yields are the integrals of the fluorescence band from 300 to 500 nm.

Bacteriorhodopsin was regenerated from bO as described previously (Huang et al., 1981; London & Khorana, 1982). Briefly, 8 μM bO in 0.4 or 0.2% SDS/50 mM sodium phosphate buffer (pH 6) was mixed with an equal volume of DMPC (2% w/v)/CHAPS (2% w/v) micelles, containing *all-trans*-retinal (added from ethanol stock, final ethanol concentration <0.5%). Final protein concentration was 4 μM, and final retinal concentration was between 0 and 8 μM. Alternatively, bO in SDS was allowed to equilibrate with DMPC/CHAPS micelles for 30 min (resulting in the formation of "bO/I_2") prior to retinal addition. Absorption and fluorescence spectra of regenerated bacteriorhodopsin were measured after overnight incubation in the dark at 22 °C. Regeneration yields were determined from the ratio of the concentration of regenerated bacteriorhodopsin to the initial concentration of bO. bO concentration was determined prior to addition of DMPC/CHAPS micelles, using an extinction coefficient for bO in SDS of 66 000 cm^{-1} M^{-1}, at 280 nm (Huang et al., 1981). The concentration of regenerated bacteriorhodopsin was determined using an extinction coefficient of 55 300 cm^{-1} M^{-1} at 555 nm (see Results). Identical regeneration yields were found for samples with final SDS concentrations of 0.1% and 0.2%.

All procedures and measurements were performed in the dark or dim light at 22 °C.

Time-Resolved Measurements. Experiments were performed using an Applied Photophysics SX.17MV stopped-flow spectrometer with a dead time of ~1.4 ms, at 22 °C. Excitation was at 290 nm (1 nm bandwidth). Emission was collected above 305 nm using a cutoff filter. Final concentrations in the stopped-flow cuvette were 2 μM protein, 1% (w/v) DMPC and CHAPS, and 0.1% (w/v) SDS.

For experiments involving initiation of protein refolding from bO, 4 μM bO in 0.2% (w/v) SDS/50 mM sodium phosphate buffer, pH 6, was mixed with an equal volume of 2% (w/v) DMPC/2% (w/v) CHAPS micelles, pH 6. Retinal was included in the micelles where indicated. Addition of retinal at various times during protein refolding involved premixing (in the stopped-flow spectrometer) 8 μM bO in 0.2% SDS/50 mM sodium phosphate buffer, pH 6, with an equal volume of 2% (w/v) DMPC/2% (w/v) CHAPS micelles, pH 6. After a preset delay time, this was rapidly mixed (by stopped-flow) with retinal in 1% DMPC, 1% CHAPS, and 0.1% SDS micelles, pH 6. Delay times between 10 ms and 30 min were used. For a delay time of 30 min, premixing of bO in SDS with DMPC/CHAPS micelles was performed manually rather than by stopped-flow. Retinal concentration was varied between 0 and 64 μM.

All procedures and measurements were performed in the dark or dim light at 22 °C.

Data Collection and Analysis. Experimentally determined rate constants (ν) were calculated by iterative reconvolution based on the Marquardt fitting algorithm, assuming multi-exponential kinetics. The quality of fits was judged by plots of the weighted residuals. Time-resolved fluorescence data were collected over several time scales (50 ms to 1000 s full scale with 4000 data points per scale, and an electronic filter about 1/10000th of the total time scale). Experimentally determined rate constants were determined from fits to data (average of 2, 4, or 16 transients) over different times: 50 ms for the fast rise; 1 s for ν_1; 50 s for ν_2 and ν_3; 10 s for ν_4 and ν_5; 1000 s for ν_6.

Data were also fit directly to a reaction scheme (see Results), in a global analysis, using the GLINT analysis program (Applied Photophysics, U.K.). Again data were fit over different time scales.

All errors are quoted to one standard deviation.

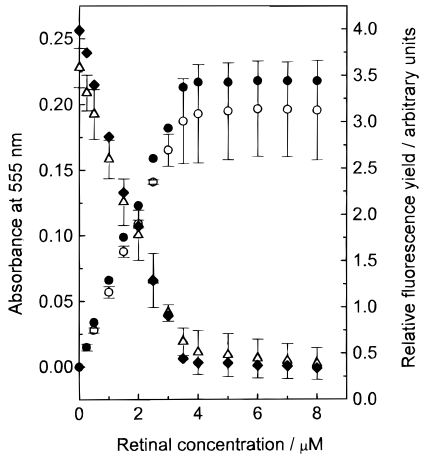

FIGURE 1: Changes in chromophore absorbance and protein fluorescence as a function of retinal concentration, on regeneration of bacteriorhodopsin. (○ and ●). Changes in absorbance at 555 nm on regeneration of bR from bO and bO/I_2, respectively. (△ and ♦). Changes in yield of protein fluorescence band on regeneration of bR from bO and bO/I_2, respectively. Each data point represents measurements on separate bO samples (from the same bO preparation), to which retinal was added simultaneously. Bacteriorhodopsin was then regenerated overnight in the dark at 22 °C, at a protein concentration 4 μM. Data for regeneration from bO are the average of three different bO preparations; error bars are shown to one standard deviation.

RESULTS

Regeneration Yields. Bacterioopsin (bO) in SDS was mixed with renaturing, DMPC/CHAPS, micelles containing retinal. Recovery of the native-like chromophore absorbance was determined after overnight incubation in the dark (see Materials and Methods). Figure 1 shows the change in chromophore absorption as a function of added retinal. Also shown are the results obtained when retinal was added to apoprotein which had been allowed to incubate in mixed DMPC/CHAPS/SDS micelles for 30 min. This latter state reflects bO in equilibrium with I_2 (see Discussion), and will be referred to as bO/I_2. In both cases, the chromophore absorption band maximum and FWHM were independent of retinal concentration, and were 554.6 ± 0.5 nm and 110 ± 2 nm, respectively (errors quoted for a 1:1 protein:retinal mole ratio). Figure 1 shows that for both bO and bO/I_2, the chromophore absorbance increases linearly with retinal concentration, until a maximum absorbance is reached. This latter absorbance reflects the maximum yield of regenerated, native-like chromophore, and hence of regenerated bacteriorhodopsin. The maximum chromophore absorbance is reached at a retinal concentration of about 3.5 μM, which is only slightly less than the bacterioopsin concentration of 4 μM. Thus, in line with previous reports (Huang et al., 1981; London & Khorana, 1982; Braiman et al., 1987), nearly all the bacterioopsin in our samples binds retinal to regenerate

Table 1: Experimentally Determined Rate Constants for Bacteriorhodopsin Regeneration

		origin of component						
				formation of apoprotein intermediate I_2		noncovalent retinal binding & formation of intermediate I_R		Schiff-base formation & regeneration of bR
process	amplitude change in deadtime[a] (%)	micelle mixing fast rise (s^{-1})[b]	formation of I_1 ν_1 (s^{-1})[b]	ν_2 (s^{-1})[b]	ν_3 (s^{-1})[b]	ν_4 (s^{-1})[b]	ν_5 (s^{-1})[b]	ν_6 (s^{-1})[b,d]
bO→bR	−109	$200_{(-14)}$	$2.2_{(4)}$	$0.14_{(69)}$[c]	$0.043_{(62)}$[c]	*[e]	*	$0.007_{(54)}$
bO→I_2	−114	$250_{(-14)}$	$7.1_{(1)}$	$0.13_{(-4)}$	$0.029_{(-15)}$	*	*	*
bO/I_2→bR		*	*	*	*	$1.6_{(64)}$[c]	$0.56_{(97)}$[c]	$0.005_{(37)}$

[a] Change in fluorescence amplitude during ∼1.5 ms mixing deadtime, i.e., difference between denatured bO in SDS and initial amplitude of bO in DMPC/CHAPS/SDS micelles, ∼1.5 ms after mixing. Amplitudes are relative to the total fluorescence amplitude change measured in the stopped-flow cuvette, from the starting state (denatured bO in SDS) to the end state (regenerated bR). [b] Experimentally determined rate constants are from fitting data (on different detection time scales) to sums of exponentials (see Materials and Methods). Relative fluorescence amplitudes, in percent, are shown, in parentheses, as subscripts to rate constants. Amplitudes are relative to the total fluorescence amplitude change from denatured bO in SDS to regenerated bR. [c] Values quoted are only a guide to the magnitude of these components. Data do not fit well to sums of exponentials, see text. [d] Values quoted are only a guide to the magnitude of this component. Measurements on a longer time scale indicated Schiff-base formation was biexponential, as previously reported. However, with 1000 s full scale, this process is adequately represented by a single exponential. The amplitude quoted is slightly less than that observed over longer time scales. [e] *, Component not detected.

bacteriorhodopsin. The binding curves essentially consist of two straight lines, which implies that in the linear region, prior to reaching the maximum absorbance, every retinal which is added binds (Rehorek & Heyn, 1979). Hence, assuming a 1:1 retinal/bacterioopsin stoichiometry, a chromophore extinction coefficient can be calculated from the gradient of the binding curve in this linear region, giving a value of 55 300 ± 800 M^{-1} cm^{-1} at 555 nm. This extinction coefficient of 55 300 M^{-1} cm^{-1} is effectively for "dark-adapted" samples, and is in good agreement with that of 56 600 M^{-1} cm^{-1} at 558 nm which has previously been reported for this refolding system (with slightly different ratios of protein, DMPC/CHAPS, and SDS) (Brouillette et al., 1989). The accuracy of the extinction coefficient for regenerated bacteriorhodopsin determined here is dependent on accurate knowledge of the concentration of retinal, rather than on accurate knowledge of either the protein concentration or the yield of regenerated bacteriorhodopsin (Rehorek & Heyn, 1979). The concentration of free retinal in ethanol was calculated using an extinction coefficient of 42 800 M^{-1} cm^{-1} at 380 nm (Rehorek & Heyn, 1979).

The yield of bacteriorhodopsin regenerated from bO was determined from the concentration of regenerated bacteriorhodopsin, compared to the initial concentration of bO (see Materials and Methods). An average of five different bO preparations gave a regeneration yield of 88 ± 16%. The spread observed in regeneration yields seems to reflect the ease with which the delipidated bO dissolved in SDS. Regeneration yields of 98 ± 2% were observed for bO preparations where the wet bO pellet dissolved in SDS after only 1 or 2 h of stirring. However, after some delipidations (even when the same batch of purple membrane was used), the wet bO pellet took longer to dissolve in SDS (up to 12 h), and this resulted in lower regeneration yields, of about 70%. An alternative method of dissolving bO in SDS involved drying down a mixture of bO and SDS in organic solvent (see Materials and Methods), and then dissolving the resulting bO/SDS powder in water. The bO/SDS mixture did not always redissolve well, and lower regeneration yields were observed if the mixture had to be stirred for several hours. All kinetic experiments reported here were performed on two or three different bO preparations which exhibited regeneration yields of 98 ± 2% (although no difference in experimentally observed rate constants was found if preparations with lower regeneration yields were used).

Figure 1 also shows the changes in the intrinsic protein fluorescence as a function of retinal concentration, when retinal was added to both bO and bO/I_2. In both cases, protein fluorescence is quenched by retinal, as a result of energy transfer from protein tryptophans to retinal (Polland et al., 1986). The fluorescence maximum was 337.1 ± 0.6 nm, and the FWHM 55.9 ± 0.3 nm (errors for a 1:1 retinal:protein mole ratio), both being independent of retinal concentration. The dependence of fluorescence yield on retinal mirrors the change in chromophore absorbance (Figure 1). As the concentration of retinal is increased, a linear decrease in fluorescence is observed until a minimum fluorescence is reached. Thus, quenching of protein fluorescence by retinal provides a convenient assay of retinal binding and bacteriorhodopsin regeneration.

Regeneration Kinetics. The kinetics of bacteriorhodopsin regeneration were determined as described previously (Booth et al., 1995). Regeneration was initiated by a rapid mixing, stopped-flow technique, and the accompanying changes in protein fluorescence were time-resolved. Table 1 shows results for three processes: overall regeneration (bO→bR), for which bO in SDS was mixed with DMPC/CHAPS micelles containing retinal (protein to retinal mole ratio 1:1); refolding in the absence of retinal (bO→I_2), for which bO in SDS was mixed with DMPC/CHAPS micelles; and retinal binding (bO/I_2→bR), for which bO in SDS was preincubated for 30 min in DMPC/CHAPS micelles, prior to mixing with DMPC/CHAPS micelles containing retinal (protein to retinal mole ratio 1:1). Table 1 shows experimentally determined rate constants obtained by fitting fluorescence data (on different time scales) to sums of exponentials (see Materials and Methods).

Data shown in Table 1 are essentially identical to those previously reported (Booth et al., 1995) for a protein:retinal ratio of 1:3, and where bO/I_2 was formed by incubation of bO in DMPC/CHAPS micelles for several hours rather than 30 min as here. In this previous study, we reported that both formation of I_2 (ν_2 and ν_3) and noncovalent retinal binding (ν_4 and ν_5) approximated to monoexponential processes. However, the higher signal to noise obtained in the data presented here (Figures 2 and 3), as a result of higher light levels, indicates that more than one exponential is required to fit the data for each process. Biexponential fits to data accompanying noncovalent retinal binding (ν_4 and ν_5), over time scales of 5 s and 10 s full scale, did not give random

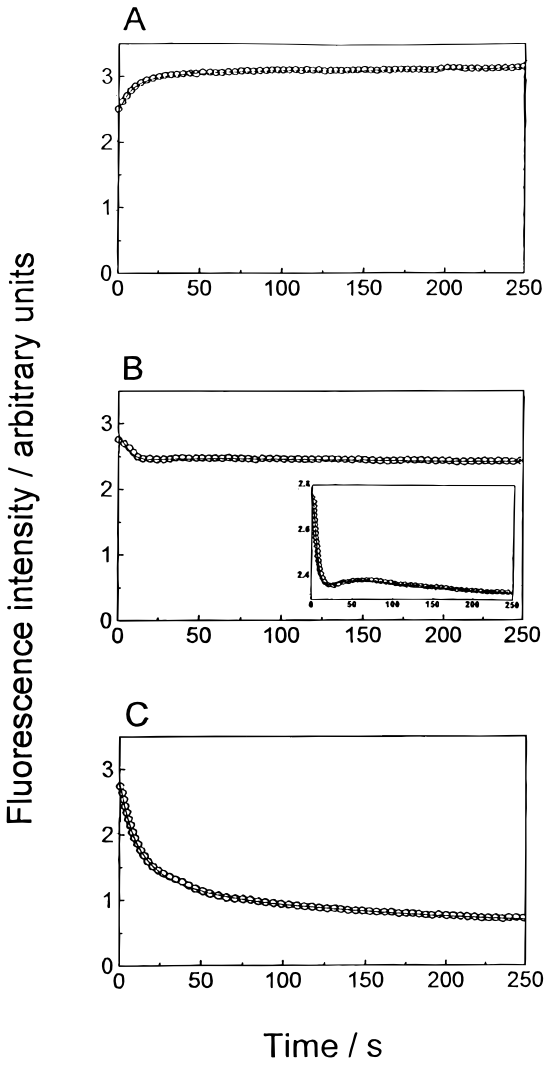

FIGURE 2: Dependence of regeneration kinetics on retinal concentration, for addition of retinal to bO. Protein to retinal mole ratios: (A) 1:0; (B) 4:1; (C) 1:1. The inset to (b) shows the *y*-axis scale expanded. Continuous line, experimental data; (○) theoretical curves obtained by modelling the experimental data with the reaction scheme given under Discussion. Experimental data collected over 1000 s, only first 250 s shown. Curves are averages of two transients. Fluorescence in arbitrary units, scales directly comparable between curves.

residuals. This reflects the second-order retinal/protein reaction under study, that is not well approximated by a sum of exponentials at a 1:1 retinal to protein ratio (see below and Discussion). Rate constants ν_4 and ν_5 are given in Table 1 only as a guide to the approximate rate of noncovalent retinal binding. Similarly, fits to data for bO→bR suggested the overall regeneration process is not correctly modelled by a sum of exponentials, again reflecting the second-order retinal binding step (see below and Discussion).

Regeneration Kinetics as a Function of Retinal Concentration. Time-resolved fluorescence curves were also measured for bacteriorhodopsin regeneration at several different retinal concentrations between 0 and 2 μM (protein to retinal mole ratios, 1:0 to 1:1), three of which are shown in Figure 2. In the absence of retinal (Figure 2A), an overall increase in fluorescence is observed reflecting formation of I_2 (Table 1, bO→I_2) (Booth et al., 1995). Increasing the concentration of retinal highlights the retinal binding step. The larger amplitude of the fluorescence quenching caused by retinal binding [as compared to the fluorescence changes associated with I_2 formation (Figure 2 and table 1)] means that binding is seen as an initial decrease in fluorescence at rate-limiting retinal concentrations (inset Figure 2B). At a 1:1 protein: retinal mole ratio (Figure 2C), an overall decrease in fluorescence is observed which corresponds to formation of bR (Table 1, bO→bR) (London & Khorana, 1982; Booth et al., 1995). Data were also collected over different time scales (ranging from 50 ms to 100 s full scale; see Materials and Methods) to investigate the effect of retinal on the faster regeneration kinetics. Retinal had no effect on either the rate constant or the amplitude of component ν_1 (data not shown).

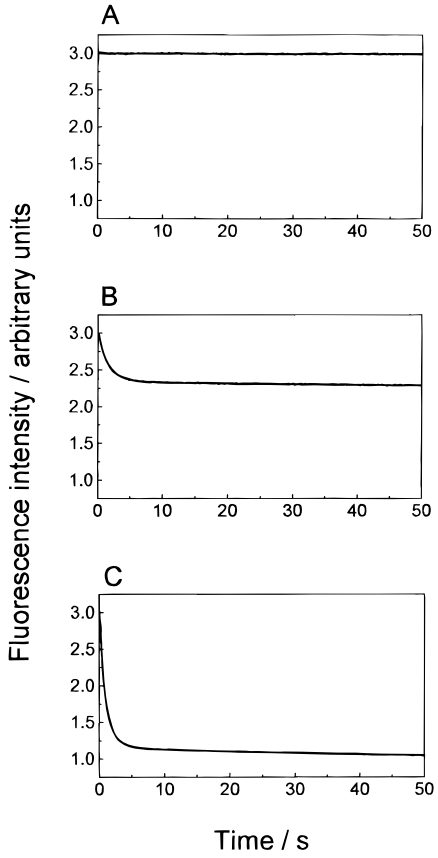

FIGURE 3: Dependence of regeneration kinetics on retinal concentration, for addition of retinal to bO/I_2 (i.e., for a delay time of 30 min). Protein to retinal mole ratios: (A) 1:0; (B) 4:1; (C) 1:1. Data collected over 50 s. Curves are averages of four transients. Fluorescence in arbitrary units, scales directly comparable between curves.

Retinal was also added at various times during the regeneration process; i.e., bO was premixed with DMPC/CHAPS micelles for a certain "delay" time prior to the addition of retinal. Delay times ranging from 0.1 s to 30 min were used, and for each delay time, the concentration of retinal was varied between protein to retinal mole ratios of 0:1 and 1:1. As above, data were collected over a range of time scales.

Addition of retinal after delays of up to 1 s gave essentially identical results to those for a zero delay time (i.e., addition of retinal to bO), except that component ν_1 was not observed with a delay time of 1 s. The results obtained with a delay time of 100 s were the same as those obtained with a delay of 30 min (Figure 3), the latter corresponding to addition of retinal to bO/I_2. Data obtained with delay times between 1 and 50 s (data not shown) agreed with the reaction scheme below.

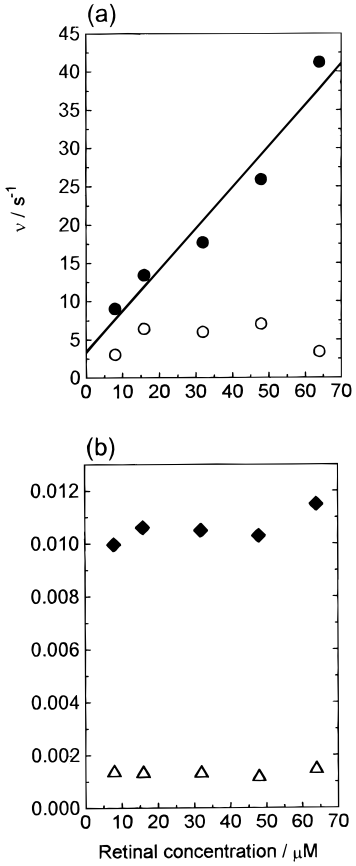

FIGURE 4: Dependence of experimentally observed rate constants for the process bO/I_2 → bR with retinal in excess. Protein to retinal mole ratios from 1:4 to 1:32, protein concentration 2 μM. (a) Experimentally observed rate constants for noncovalent retinal binding: (●) ν_4; (○) ν_5. Straight line represents a linear fit to ν_4. (b) Experimentally observed rate constants for covalent retinal binding, (△) ν_6; (♦) ν_7.

The dependence of the kinetics accompanying bO/I_2→bR (i.e., for a delay of 30 min) on retinal was also determined when retinal was in excess (protein to retinal mole ratios ranging from 1:4 to 1:32). Biexponential kinetics have previously been reported for Schiff-base formation (Huang et al., 1981; London & Khorana, 1982; Booth et al., 1995). In order to determine the dependence of both of these experimentally determined rate constants on retinal, data reflecting Schiff-base formation were fit to two exponentials (ν_6 and ν_7). Figure 4 shows the dependence of the experimentally observed rate constants for noncovalent retinal binding (ν_4 and ν_5) and Schiff-base formation (ν_6 and ν_7) on retinal concentration.

DISCUSSION

Yield of Regenerated Bacteriorhodopsin. Functional bacteriorhodopsin is characterized by its ability to pump protons across a membrane or lipid bilayer in response to illumination (Stoeckenius & Bogomolni, 1982; Oesterhelt & Tittor, 1989; Birge, 1990). It has previously been reported that bacteriorhodopsin regenerated in DMPC/CHAPS/SDS micelles exhibits the characteristic photoreactions of the proton pumping cycle (Braiman et al., 1987), and this is reflected in a native-like chromophore absorption band. The extent of recovery of a native-like chromophore absorption band on regeneration of bacteriorhodopsin therefore provides a convenient measure of the yield of regenerated bacteriorhodopsin (Oesterhelt & Schuhmann, 1974; Huang et al., 1981). The yield of bacteriorhodopsin, regenerated from a denatured state in SDS in renaturing DMPC/CHAPS micelles, at pH 6 and 22 °C, is 88 ± 16%, in agreement with previous studies (Huang et al., 1981; London & Khorana, 1982; Braiman et al., 1987). Addition of retinal later during bacteriorhodopsin regeneration (e.g., after 30 min, to bO/I_2) results in an identical regeneration yield.

A spread in regeneration yield is observed between different bO preparations which seems to result from the delipidation process and subsequent SDS solubilization: about 95% regeneration is found if the delipidated bO dissolves readily in SDS; otherwise, lower yields are observed. Therefore, the small percentage of protein which does not regenerate bacteriorhodopsin most likely represents an irreversibly aggregated state in SDS, which does not contribute to the observed regeneration kinetics. Alternatively, one (or more) of the kinetic components we observe may correspond to formation of an aggregated/misfolded state which cannot regenerate bacteriorhodopsin (indeed the latter may be the origin of ν_5), or to heterogeneity in protein preparations.

Reaction Scheme for Regeneration of Bacteriorhodopsin. Several kinetic phases are observed on regeneration of bacteriorhodopsin. In order to determine which phases are dependent on retinal, and reflect a reaction between retinal and protein, we have studied the regeneration kinetics at different retinal concentrations. Previous work has suggested that a slow protein folding step precedes retinal binding (London & Khorana, 1982), which makes the latter process difficult to resolve when retinal is added to bacterioopsin at the start of regeneration (Booth et al., 1995). In order to overcome this difficulty, we have also added retinal at various times during regeneration, and investigated the reaction of retinal with each transient intermediate involved in bacteriorhodopsin regeneration.

The data presented here support the following reaction scheme (Figure 2):

$$\mathrm{bO} \underset{k_{-1}}{\overset{k_1}{\rightleftharpoons}} \mathrm{I_1} \underset{k_{-2}}{\overset{k_2}{\rightleftharpoons}} \mathrm{I_2} \underset{k_{-3}}{\overset{\mathrm{R},\,k_3}{\rightleftharpoons}} \mathrm{I_R} \xrightarrow{k_4} \mathrm{I_3} \xrightarrow{k_5} \mathrm{bR}$$

where R is retinal, bR, regenerated bacteriorhodopsin, and all rate constants are first order, except k_3, which is the second-order, retinal binding rate constant, and $k_1 = 2\ s^{-1}$, $k_{-1} = 0.01\ s^{-1}$, $k_2 = 0.06\ s^{-1}$, $k_{-2} = 0.008\ s^{-1}$, $k_3 = 0.54\ s^{-1}\ \mu M^{-1}$, $k_{-3} = 3.3\ s^{-1}$, $k_4 = 0.009\ s^{-1}$, and $k_5 = 0.003\ s^{-1}$. Values for rate constants were obtained from fits to data collected over different time scales; for example, k_1 was obtained from fits to data with 500 ms full scale (see Materials and Methods). Values for k_3 and k_{-3} were obtained from Figure 4 (see Discussion). Schiff-base formation is represented, for simplicity, as two sequential steps, k_4 and k_5, in line with previous reports of biexponential kinetics for this step (Huang et al., 1981; London & Khorana, 1982), and only on this basis do we invoke an intermediate, I_3. Back-reactions for these last two steps are assumed negligible (see below). Data for addition of retinal to bO/I_2 (Figure 3) could be modelled by the last three steps of the above scheme; earlier steps were assumed negligible as the equilibrium between bO and I_2 had been established. There was also evidence for a faster event [possibly correspondsing to

$k(\text{obs})_5$], and good fits of data with bO/I_2 as the starting point to the above reaction scheme were only obtained when the first 200 ms was ignored.

One of the key features of the above reaction scheme is that formation of I_2 is slower than subsequent retinal binding (k_2 is about 0.06 s^{-1}, whereas k_3 is about 0.54 s^{-1} μM^{-1}; Figure 2). This slow formation of I_2 makes it difficult to resolve the rate constant associated with the subsequent retinal binding, as well as the nature of the dependence of this latter rate constant on retinal concentration. Addition of retinal after the equilibrium between bO and I_2 is established (i.e., addition of retinal to bO/I_2) allows the retinal binding step to be clearly observed. Increasing the concentration of retinal added to bO/I_2 results in an increase in the amplitude of the fluorescence quenching which accompanies retinal binding (Figure 3).

In the simplest case, the reaction of retinal and bO/I_2

$$(bO/I_2) + R \underset{k_{-3}}{\overset{k_3}{\rightleftharpoons}} I_R \qquad (1)$$

follows second-order kinetics. When retinal is in excess, this reaction will exhibit pseudo-first-order kinetics, which simplifies the integrated rate law to (Fersht, 1985)

$$\nu = k_{-3} + k_3[R] \qquad (2)$$

Hence, the experimentally observed rate constant, ν, for the retinal/protein reaction will increase linearly with retinal concentration. The studies reported here, with excess retinal, show that only one experimentally observed rate constant, ν_4, exhibits a linear dependence on retinal concentration (Figure 4a), identifying it as the second-order retinal binding step. This rate corresponds to that previously assigned to formation of a noncovalent retinal/protein intermediate, I_R (Booth et al., 1995). As expected from our reaction scheme, and as previously reported (London & Khorana, 1982), neither of the rates observed for Schiff-base formation vary with retinal concentration (Figure 4b).

Therefore, we find only one experimentally determined rate constant (ν_4) to be dependent on retinal. No dependence on retinal was found for the process $bO \rightarrow I_1$, and identical results were found whether retinal was added to bO, during the reaction $bO \rightarrow I_1$, or effectively to I_1 (i.e., for delays of up to 1 s). Hence, we find no evidence that retinal binds to either bO or I_1. The experiments reported here are reliant on identification of retinal binding through quenching of protein fluorescence. It is possible that there is more than one retinal binding step, but for some reason it is not accompanied by quenching of protein fluorescence. However, preliminary absorption data, which follow the changes in the absorption band of retinal during bacteriorhodopsin regeneration, are also consistent with the reaction scheme reported here (unpublished results).

Thermodynamics of Retinal Binding. Values for the second-order rate constant, k_3, for retinal binding and the first-order retinal dissociation constant, k_{-3}, can be calculated from Figure 4a using eq 2. Values of 0.54 s^{-1} μM^{-1} and 3.3 s^{-1} are obtained for k_3 and k_{-3}, respectively. The equilibrium constant, K, for the retinal binding reaction shown in eq 1 can be calculated from k_3/k_{-3} as 0.16 μM^{-1}, giving a ΔG of -30 kJ·mol^{-1} (at pH 6 and 295 K). The main assumption in this calculation is that the reaction shown in eq 1 can be treated as a quasi-static equilibrium. This is likely to be true with regard to depopulation of the equilibrium through formation of bacteriorhodopsin, as this latter process occurs with rate constants orders of magnitudes slower than k_3 and k_{-3}. It is also assumed that bO is in equilibrium with I_2. Again, this is a reasonable assumption since we obtain essentially identical results for addition of retinal to bO which has been allowed to equilibrate with I_2 for 100 s, 30 min, or several hours. In future studies, we shall investigate the equilibrium between bO and I_2 in more detail.

An enthalpy change of about -400 kJ·mol^{-1} has been reported for the equilibrium between apoprotein and bR, in lipid vesicles, where apoprotein was formed by bleaching bacteriorhodopsin (Kahn et al., 1992). The free energy change of -30 kJ·mol^{-1} reported here relates to the equilibrium between bO/I_2 and the intermediate I_R (where retinal is noncovalently bound). Although the two apoprotein states, bO/I_2 and the bleached state of bacteriorhodopsin, are not necessarily equivalent, a comparison of our free energy change, of -30 kJ·mol^{-1}, with the enthalpy change of -400 kJ·mol^{-1} (assuming a negligible, or favorable, entropy contribution) suggests that further stabilization of bacteriorhodopsin occurs during Schiff-base formation, when retinal binds covalently in its pocket.

A theoretical model has been proposed for the folding of helical membrane proteins, largely based on earlier renaturation experiments on bacteriorhodopsin (Popot et al., 1987; Popot & Engelman, 1990). In this model, the folding problem is simplified to two stages; first, inherently stable transmembrane helices form, and second, these helices pack together to give functional protein. In terms of this model, the kinetics discussed here most likely relate to the second, helix-packing, stage. Factors which may drive transmembrane helix association include retinal binding, external constraints provided by helix-connecting loops, and packing effects (helix−helix and lipid−lipid packing being favored over helix−lipid packing) (Popot & Engelman, 1990; Lemmon & Engelman, 1994). Of these, the latter is thought to be the predominant driving force for transmembrane helix association (Lemmon & Engelman, 1994). Extramembranous loops are thought to be relatively unimportant, and indeed it is possible to regenerate bacteriorhodopsin even when one or two of the extramembranous loops are cleaved (Huang et al., 1981; Liao et al., 1983; Popot et al., 1987). Not only can bacterioopsin fold in the absence of retinal to a state with native secondary structure (London & Khorana, 1982), but also retinal binding has been found to make only a small contribution to bacteriorhodopsin's stability, its contribution being about the same as that of two of the extramembranous loops (Kahn et al., 1992). These earlier results, together with the data presented here, suggest that although retinal binding does not initiate protein folding nor is a major driving force for helix association, it is the driving force for regeneration of bacteriorhodopsin from partially folded apoprotein (I_2). In the absence of retinal, an equilibrium is established between bO and I_2, and it is retinal binding which drives the reaction to completion. How the structure of I_2 relates to that of bacteriorhodopsin is currently under investigation.

CONCLUSION

The retinal binding studies presented here detect only one second-order reaction, which reflects binding of retinal to partially folded apoprotein, and allows the free energy change for this binding to be estimated. Thus, it is possible to obtain thermodynamic information on transient intermediates involved in regeneration of a membrane protein. Further studies should allow us to build up a more complete picture of the energetics of the regeneration process for bacteriorhodopsin. When coupled with site-directed mutagenesis methods (Braiman et al., 1987; Khorana, 1988; Soppa & Oesterhelt, 1989; Krebs et al., 1991), this opens the way for mapping out structures of intermediates involved in bacteriorhodopsin regeneration, as has been elegantly shown for water-soluble proteins (Matouschek et al., 1990).

ACKNOWLEDGMENT

We thank David Klug for helpful discussions and critical reading of the manuscript, and Mark Fricker, Alison Telfer, and James Barber for help with steady-state fluorescence and absorption measurements. We are also grateful to Tony Watts and David Harris for their interest and support.

REFERENCES

Birge, R. R. (1990) *Biochim. Biophys. Acta 1016*, 293−327.
Booth, P. J., Flitsch, S. L., Stern, L. J., Greenhalgh, D. A., Kim, P. S., & Khorana, H. G. (1995) *Nat. Struct. Biol. 2*, 139−143.
Braiman, M. S., Stern, L. J., Chao, B. H., & Khorana, H. G. (1987) *J. Biol. Chem. 262*, 9271−9276.
Brouillette, C. G., McMichens, R. B., Stern, L. J., & Khorana, H. G. (1989) *Proteins: Struct., Funct., Genet. 5*, 38−46.
Bycroft, M., Matouschek, A., Kellis, J. T., Jr., Serrano, L., & Fersht, A. R. (1990) *Nature 346*, 488−490.
Donnelly, D., & Findlay, J. B. C. (1994) *Curr. Opin. Struct. Biol. 4*, 582−589.
Eisele, J.-L., & Rosenbuch, J. P. (1990) *J. Biol. Chem. 265*, 10217−10220.
Fersht, A. (1985)*Enzyme structure and mechanism*, W. H. Freeman & Co., New York.
Hargrave, P. A. (1991) *Curr. Opin. Struct. Biol. 1*, 575−581.
Henderson, R., Baldwin, J. M., Ceska, T. A., Zemlin, F., Beckmann, E., & Downing, K. H. (1990) *J. Mol. Biol. 213*, 899−929.
Huang, K.-S., Bayley, H., Liao, M.-J., London, E., & Khorana, H. G. (1981) *J. Biol. Chem. 256*, 3802−3809.
Kahn, T. W., Sturtevant, J. M., & Engelman, D. M. (1992) *Biochemistry 31*, 8829−8839.
Khorana, H. G. (1988) *J. Biol. Chem. 263*, 7439−7442.
Khorana, H. G. (1993) *Proc. Natl. Acad. Sci. U.S.A. 90*, 1166−1171.
Krebs, M. P., Hauss, T., Heyn, M. P., Rajbhandary, U. L., & Khorana, H. G. (1991) *Proc. Natl. Acad. Sci. U.S.A. 88*, 859−863.
Lemmon, M. A., & Engelman, D. M. (1994) *Q. Rev. Biophys. 27*, 157−218.
Liao, M.-J., London, E., & Khorana, H. G. (1983) *J. Biol. Chem. 258*, 9949−9955.
London, E., & Khorana, H. G. (1982) *J. Biol. Chem. 257*, 7003−7011.
Matouschek, A., Kellis, J. T., Jr., Serrano, L., Bycroft, M., & Fersht, A. R. (1990) *Nature 346*, 440−445.
Matthews, C. R. (1993) *Annu. Rev. Biochem. 62*, 653−683.
Oesterhelt, D., & Schuhmann, L. (1974) *FEBS Lett. 44*, 262−265.
Oesterhelt, D., & Stoeckenius, W. (1974) *Methods Enzymol. 31*, 667−679.
Oesterhelt, D., & Tittor, J. (1989) *Trends Biochem. Sci. 14*, 57−61.
Oprian, D. D. (1992) *J. Bioenerg. Biomembr. 24*, 211−217.
Paulsen, H., Rümler, U., & Rüdiger, W. (1990) *Planta 181*, 204−211.
Plumley, F. G., & Schmidt, G. W. (1987) *Proc. Natl. Acad. Sci. U.S.A. 84*, 146−150.
Polland, H. J., Franz, M. A., Zinth, W., Kaiser, W., & Oesterhelt, D. (1986) *Biochim. Biophys. Acta 851*, 407−415.
Popot, J.-L., & Engelman, D. M. (1990) *Biochemistry 29*, 4031−4037.
Popot, J.-L., Gerchman, S.-E., & Engelman, D. M. (1987) *J. Mol. Biol. 198*, 655−676.
Rehorek, M., & Heyn, M. P. (1979) *Biochemistry 18*, 4977−4983.
Savarese, T. M., & Fraser, C. M. (1992) *Biochem. J. 283*, 1−19.
Schertler, G. F. X., Villa, C., & Henderson, R. (1993) *Nature 362*, 770−772.
Soppa, J., & Oesterhelt, D. (1989) *J. Biol. Chem. 264*, 13043−13048.
Stoeckenius, W., & Bogomolni, R. A. (1982) *Annu. Rev. Biochem. 52*, 587−616.

BI960129E